MOLECULAR IMAGING AND BIOLOGY

Mol Imaging Biol (2019) 21:232–239
DOI: 10.1007/s11307-018-1243-6

Published Online: 27 June 2018

RESEARCH ARTICLE

In Vivo Mapping and Quantification of Creatine Using Chemical Exchange Saturation Transfer Imaging in Rat Models of Epileptic Seizure

Dong-Hoon Lee,[1] Do-Wan Lee,[2] Jae-Im Kwon,[3] Chul-Woong Woo,[3] Sang-Tae Kim,[3] Jin Seong Lee,[4] Choong Gon Choi,[4] Kyung Won Kim,[4] Jeong Kon Kim,[4] Dong-Cheol Woo[3,5]

[1]*Faculty of Health Sciences and Brain & Mind Centre, The University of Sydney, Sydney, NSW, Australia*
[2]*Center for Bioimaging of New Drug Development, and MR Core Laboratory, Asan Medical Center, Asan Institute for Life Sciences, Seoul, Republic of Korea*
[3]*MR Core Laboratory, Asan Medical Center, Asan Institute for Life Sciences, 88, Olympic-ro 43-gil, Songpa-gu, Seoul, 138-736, Republic of Korea*
[4]*Department of Radiology, Asan Medical Center, University of Ulsan College of Medicine, Seoul, Republic of Korea*
[5]*Department of Convergence Medicine, Asan Medical Center, University of Ulsan College of Medicine, Seoul, Republic of Korea*

Abstract

Purpose: To evaluate signal changes in the hippocampus of epileptic seizure rat models, based on quantified creatine chemical exchange saturation transfer (CrCEST) signals.

Procedures: CEST data and ^{1}H magnetic resonance spectroscopy (^{1}H MRS) data were obtained for the two imaging groups: control (CTRL) and epileptic seizure-induced (ES; *via* kainic acid [KA] injection) groups. CrCEST signals in the hippocampal regions were quantitatively evaluated; correlations between CrCEST signals and phosphocreatine (PCr) and total creatine (tCr; PCr + Cr) concentrations, derived from the analysis of ^{1}H MRS data, were investigated as a function of time changes (before KA injection, 3 and 5 h after KA injection).

Results: Measured CrCEST signals were exhibited significant differences between before and after KA injection in the ES group. At each time point, CrCEST signals showed significant correlations with PCr concentration (all $|r| > 0.59$; all $P < 0.05$); no significant correlations were found between CrCEST signals and tCr concentrations (all $|r| < 0.22$; all $P > 0.05$).

Conclusions: CrCEST can adequately detect changes in the concentration of Cr as a result of energy metabolism, and may serve as a potentially useful tool for diagnosis and assessment of prognosis in epilepsy.

Key words: Creatine, Chemical exchange saturation transfer, Phosphocreatine, Epilepsy, Magnetic resonance spectroscopy

Introduction

Epilepsy is the most common neurological brain disorder, characterized by disruptions in the balance between cerebral excitation and inhibition, which leads to spontaneous seizures that can cause severe cognitive and social

Dong-Hoon Lee and Do-Wan Lee contributed equally to this work.

Correspondence to: Dong-Cheol Woo; *e-mail:* dcwoo@amc.seoul.kr

impairments [1–4]. Because epileptic seizures can have a detrimental effect on the brain or health-related social activities as well as be caused by various conditions and reasons, many studies are still underway to understand the mechanisms underlying epileptic seizures, with the aim of improving treatment strategies [5–7]. Thus far, in order to localize the epileptic activity or epileptogenic region by the metabolic characteristics of epileptic brain, many medical imaging systems have been used, including magnetic resonance imaging (MRI) [5–8], single-photon emission computed tomography [9–12], and 2-deoxy-2-[^{18}F]fluoro-D-glucose positron emission tomography [13, 14]. Notably, *in vivo* studies using MRI have enabled tracking of the evolution of structural brain changes in epilepsy *via* sensitive detection of water protons in T2-weighted images [15–17]. In addition to the gross morphological features shown in MRI, chemical composition changes can be detectable *via* proton MR spectroscopy (^{1}H MRS), using concentration changes in brain metabolites, such as N-acetylaspartate (NAA) and glutamate (Glu) [3, 18–20]. These types of metabolites have been used as effective biomarkers to define epilepsy and its biological changes. Interestingly, during seizures, the glycolytic pathway enhances to anaerobic metabolism, intracellular acidosis, and depletion of adenosine triphosphate (ATP). In terms of ATP changes during seizures, creatine (Cr) is regarded as an important energy metabolite because it increases the Cr phosphate pool, which can accelerate the energy generation of ATP to satisfy the demands of high energy consumption of brain tissues [21–23]. Thus, Cr plays a major role in the storage and transmission of phosphate-bound energy; variation of Cr levels can be considered as a useful indicator to clinically evaluate brain energy metabolism in epilepsy.

In recent years, chemical exchange saturation transfer (CEST)-MRI, a new contrast enhancement technique, has become available to indirectly detect the molecules with exchangeable protons and exchange-related properties [24–27]. The CEST-MRI can detect vital tissue metabolites by using differences between with and without saturation of the solute pool. The difference decreases proportionally in the water signal resulting from the accumulation of saturated protons in the bulk water pool, when a frequency-selective radio frequency (RF) is applied. Cr can be measured based on well-known theories and experimental results, which show a concentration-dependent CEST effect between amine ($-NH_2$) and bulk water protons; its amine protons demonstrate an exchange rate of approximately 1.8 ppm from water [25, 26].

The aim of this study is to demonstrate the usefulness of the CrCEST effect in kainic acid (KA)-induced rat model to detect and define epilepsy by mapping the energy metabolites in the hippocampus. More specifically, metabolite characteristics presented in KA-induced epileptic seizure were evaluated by the CrCEST signal features, and the signals were performed correlation analysis with the phosphocreatine (PCr) and total Cr (tCr; PCr + Cr) concentrations that measured by ^{1}H MRS.

Materials and Methods

Kainic Acid-Induced Rat Model of Epilepsy

This study was performed in strict accordance with the recommendations as per the guidelines of the Care and Use of Laboratory Animals of the National Institutes of Health. The protocol was approved by the University of Ulsan Animal Care and Use Committee (Permit Number: 2016-13-236). To evaluate the CrCEST effect in KA-induced rat model of epilepsy, the male Wistar rats (250–300 g, Orient Bio Inc., Seongnam, Kyunggi-do, Republic of Korea) were divided into two groups as follows: epileptic seizure group (ES group, $N = 7$) which received 15 mg/kg for KA *via* intraperitoneal injection [20, 28], and control group (CTRL group, $N = 7$) which received saline in an identical manner. The all rats were anesthetized with 1.5–3.0 % isoflurane for induction and 2.0 % for maintenance during the scanning. In all procedures, the respiration of the rat was monitored online using a small-animal respiratory-gating system (SA Instruments Inc., Stony Brook, NY, USA), and the temperature was maintained at approximately 37 °C using a warm-water circulating flat-bed positioned around its body. However, two rats were excluded from the ES group because of severe motion artifacts in scanning and data analysis despite using the immobilization and the motion correction process, respectively. Thus, each of five rats was finally analyzed for the ES and the CTRL group to match the number of rats.

MRI and MRS Data Acquisitions

All MR imaging and MR spectroscopy were performed using a horizontal 7.0 T/160 mm *in vivo* scanner (Bruker PharmaScan 70/16, Bruker BioSpin GmbH, Germany), with 400 mT/m gradient sets. After acquiring baseline data prior to KA injection, all scans were conducted at 3 and 5 h after KA administration.

For CrCEST data, a Turbo-Rapid Acquisition with Relaxation Enhancement (RARE) at 25 different frequency offsets (S_0 image as reference scan and + 3.96 to − 3.96 ppm with an interval of 0.33 ppm) was used with the following scanning parameters: repetition time (TR) = 4200 ms, echo time (TE) = 36.4 ms, echo spacing = 6.1 ms, RARE factor = 16, field of view (FOV) = 30 × 30 mm^2, matrix size = 96 × 96, and slice thickness = 1 mm. A continuous-wave RF saturation pulse was irradiated with power of 5.6 μT and saturation duration of 4 s.

To correct B_0 and B_1 field inhomogeneities, B_0 maps with double echo-times (1.9 and 2.6 ms) and B_1 maps with double flip-angles (30 and 60 °) were collected after CEST dataset acquisition [29, 30].

Water-suppressed *in vivo* ^{1}H MRS spectra were obtained using a spin-echo-based point-resolved spectroscopy (PRESS) pulse sequence, with variable power and optimized relaxation delays (VAPOR) method (TR = 5000 ms, TE =

16.3 ms, spectral width = 5000 Hz, 128 acquisitions, and number of data points = 2048) [31]. The center of the volume of interest ($2.0 \times 2.0 \times 3.0$ mm^3; 12.0 µl) located in the hippocampal region was positioned + 2.0 mm midline, − 4.0 mm from the bregma, and + 3.0 mm from the skull surface. Voxel coordinates were determined according to the atlas of the rat brain [32].

Data Analysis

Raw CEST data with KA injected was registered to non-KA injected CEST imaging using a six-degree-of-freedom rigid body transformation.

The B_0 map was calculated by linearly fitting the accumulated phase per pixel for the phase difference ($\Delta\theta_0$) against the difference of TE (ΔTE) by using Eq. (1) [29].

$$B_0 = \frac{\Delta\theta_0}{\Delta\mathrm{TE}} \tag{1}$$

For B_1 map, flip angle maps were first generated by solving Eq. (2) [29],

$$\frac{S(2\theta)}{S(\theta)} = \frac{\cos(2\theta)}{\cos(\theta)} \tag{2}$$

where $S(\theta)$ and $S(2\theta)$ denote the pixel signals in an image with preparation flip angle θ and 2θ, respectively.

From the flip angle map, the final B_1 map can be calculated by Eq. (3),

$$B_1 = \frac{\rho}{360\tau} \tag{3}$$

where ρ and τ denote the calculated flip angle map from Eq. (2), and preparation pulse duration (τ; 1 ms in this study), respectively.

The Z-spectrum derived by correcting the field homogeneity was used to analyze the magnetization transfer ratio asymmetry ($\mathrm{MTR_{asym}}$) at frequency offset ($\Delta\omega$), as follows Eq. (4),

$$\mathrm{MTR_{asym}}(\Delta\omega) = \frac{S_{\mathrm{sat}}(-\Delta\omega) - S_{\mathrm{sat}}(+\Delta\omega)}{S_0} \tag{4}$$

where S_0 and S_{sat} denote the signal intensities without and with saturation pulse, respectively.

The CrCEST contrast map ($\mathrm{CrCEST_{map}}$) was computed by subtracting the normalized signals at the 1.65 and 1.98 ppm, from the symmetric signals at the corresponding reference frequencies at the upfield from the water. In this study, we averaged two $\mathrm{MTR_{asym}}$ signals at the 1.65 and 1.98 ppm to define the CrCEST signal location, and also acquired $\mathrm{CrCEST_{map}}$ using averaged signals pixel-by-pixel.

To quantify the signal values on the $\mathrm{CrCEST_{map}}$, two regions of interest (ROIs) were set in the left and right hippocampus regions.

^{1}H MRS spectra were analyzed with a fully blind spectral process, using Linear Combination Model (LCModel) software (Version 6.2-1 L, Stephen Provencher Incorporated, Oakville, Canada) with a simulated basis set including 18 metabolites, as follows: alanine (Ala), aspartate (Asp), myo-inositol (mIns), Cr; gamma-aminobutyric acid (GABA), PCr, Glu, glutamine (Gln), glucose (Glc), scyllo-inositol (sI), glycine (Glyc), glycerophosphocholine (GPC), lactate (Lac), N-acetylaspartylglutamate (NAAG), NAA, glutathione (GSH), phosphocholine (PCh), taurine (Tau), total NAA = NAA + NAAG, Glx = Glu + Gln, tCr, and total Cho = GPC + PCh. All signal intensities from the *in vivo* basis set were processed with water referencing and eddy current correction, and metabolite concentrations were calculated (µmol/g). All metabolite peaks were fitted in the chemical shift range, from 0.3 to 4.3 ppm.

Statistical Analysis

For statistical analysis, the Mann-Whitney U test was used to compare the ES and CTRL groups at each time point. Within each group, multiple comparisons between each time point were performed with the non-parametric Friedman test, followed by *post hoc* analysis using the Wilcoxon signed-rank test for pairwise comparison. A P value of < 0.05 was considered to be significant in all statistical analyses. For the correlation analysis between the CrCEST signals and PCr and total Cr concentrations, Spearman's rank correlation coefficient (r) and P values were calculated. All CrCEST-related image processing and correlation analysis was performed using in-house-written MATLAB R2014a (The MathWorks, Inc., Natick, MA) scripts, and statistical tests were performed with PASW statistics (version 18.0, SPSS Inc., Chicago, IL).

Results

Figure 1 shows the $\mathrm{MTR_{asym}}$ curves between each group for time changes before and after KA injection. Before KA injection, the $\mathrm{MTR_{asym}}$ curves showed no significant differences between ES and CTRL groups (Fig. 1a), indicating that the values from two groups exhibit stable status with the deviation around 1 % (4.61 ± 1.03 *vs.* 5.67 ± 0.85 % at 1.65 ppm; 5.52 ± 0.58 *vs.* 6.76 ± 0.82 % at 1.98 ppm, ES and CTRL group, respectively). In addition, when $\mathrm{MTR_{asym}}$ of the left and the right hippocampus was compared, there was no significant difference in each group ($P > 0.05$). However, after KA injection, the CrCEST signals in the ES group increased (Fig. 1b) relative to the CTRL group until 5 h after KA injection (Fig. 1c), as expected (8.27 ± 1.28~9.77 ± 0.64 %/6.11 ± 0.76~7.21 ± 0.38 % for ES group and CTRL group at 3 h, respectively, and 7.07 ± 1.17~8.88 ± 1.28 %/6.54 ± 0.96 %~7.46 ± 0.59 % for ES

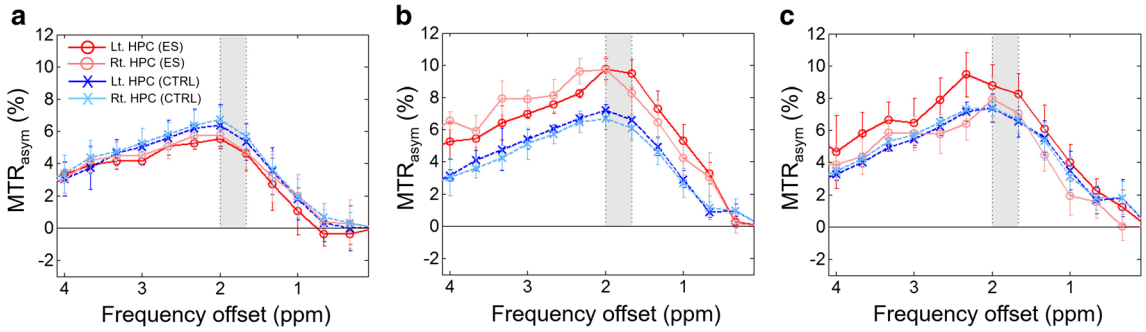

Fig. 1. Creatine CEST (CrCEST) signal features and conventional magnetisation transfer ratio asymmetry (MTR_{asym}) spectra as a function of time, **a** before, **b** 3 h, and **c** 5 h after kainic acid (KA) injection. Gray color indicates the point from 1.65 to 1.98 ppm used for the quantification of CrCEST. (Lt. HCP hippocampus at left hemisphere, Rt. HCP hippocampus at right hemisphere, ES epileptic seizure group by KA injection, and CTRL control group).

group and CTRL group at 5 h, respectively; all values indicated the minimum and maximum values at hippocampus on right and left hemisphere between two frequency offsets). Interestingly, the CrCEST signals at 5 h after KA injection were reduced, compared with those at 3 h, although the signals of the ES group were higher than the CTRL group until 5 h.

Figure 2 shows the calculated CrCEST signals that were averaged between two frequency offsets between each group for time changes. All values are summarized in Table 1. The CrCEST signals of the ES group in the left hippocampus (Fig. 2a) indicated that the signal increased significantly (9.8 ± 0.8 % at 3 h, and 8.5 ± 1.2 % at 5 h), compared with the CTRL group. There were statistically significant differences between the two groups after KA injection (all $P = 0.009$). The CrCEST signals of the ES group in the right hippocampus (Fig. 2a) indicated that the signal increased significantly (8.9 ± 2.9 % at 3 h, and 7.5 ± 2.5 % at 5 h) compared with the CTRL group, similar to the values in the left hippocampus. There was also a statistical difference between the two groups after KA injection ($P = 0.009$ at 3 h). In addition, the statistical analysis of CrCEST signals between both hippocampus regions showed no significant differences within each group ($P > 0.05$). Overall, in both hippocampus regions of the ES group (Fig. 2a, b), the quantified CrCEST signals showed statistically significant differences among all time points ($\chi^2 = 10.000$; $P = 0.007$ with *post-hoc* all $P < 0.043$ on left hippocampus, and $\chi^2 = 8.400$; $P = 0.015$ with *post-hoc* all $P < 0.043$ on right hippocampus), while those signals in the CTRL group were not significant ($P > 0.05$). In both hippocampus regions of the ES group (Fig. 2a, b), the quantified CrCEST signals at 5 h after injection were slightly decreased, compared with those at 3 h after injection. However, the results showed statistically significances in comparisons among all time points ($\chi^2 = 10.000$; $P = 0.007$ with *post-hoc* all $P < 0.043$ on left hippocampus, and $\chi^2 = 8.400$; $P = 0.015$ with *post-hoc* all $P < 0.043$ on right hippocampus), while those signals in the CTRL group were not significant ($P > 0.05$). The comparisons of CrCEST contrast (Fig. 2c) showed the distinct difference in values after 3 and 5 h, compared with before injection (-0.59 ± 1.48 %/-0.96 ± 1.17 %, 2.73 ± 0.69 %/2.57 ± 1.98 %, and 1.37 ± 1.01 %/0.44 ± 1.55 % at before injection, as well as 3 and 5 h after injection on left/right hippocampus, respectively). The contrast values within each hippocampus were statistically significantly different ($\chi^2 = 18.200$; $P = 0.000$ with *post-hoc* all $P < 0.007$ on left hippocampus, and $\chi^2 = 13.400$; $P = 0.001$ with *post-hoc* all $P < 0.037$ on right hippocampus), but there was no difference in the comparisons between hippocampi (all $P > 0.131$).

Figure 3 shows the correlation results between CrCEST signals and PCr and total Cr (PCr + Cr) concentrations at the left hippocampus region in terms of the elapsed time after KA injection. The CrCEST signals after KA injection were relatively increased, compared with the signal of pre-injection as mentioned in Fig. 2, whereas the PCr concentration was decreased (3.55 ± 0.28, 3.13 ± 0.39, and 2.59 ± 0.49 μmol/g at each time point, respectively). The strong correlation (all $|r| > 0.59$; all $P < 0.05$) was observed as in Fig. 3a. In contrast to PCr, the total Cr concentration (6.33 ± 0.21, 6.57 ± 0.91, and 6.31 ± 0.46 μmol/g at each time point, respectively) showed no significant correlations (all $|r| < 0.22$; all $P > 0.05$, Fig. 3b), despite the increase in CrCEST signal.

Figure 4 shows the reconstructed $CrCEST_{map}$ in both hippocampus regions of ES and CTRL groups over all time periods. Whereas both hippocampus presented hyperintensities in the ES group (Fig. 4a) as compared to pre-injection of KA in $CrCEST_{map}$, there was no signal difference in the CTRL group (Fig. 4b).

Discussion

Cr is well-known as a factor that plays an essential role for energy metabolism as an active form of PCr [21, 23]. In ATP synthesis, such as the PCr + ADP ↔ ATP + Cr relationship, PCr acts as a donor of high energy phosphate molecules to adenosine diphosphate (ADP) to form ATP. ATP is also a phosphate donor and supplies energy for energy-requiring processes. Thus, PCr is broken down by

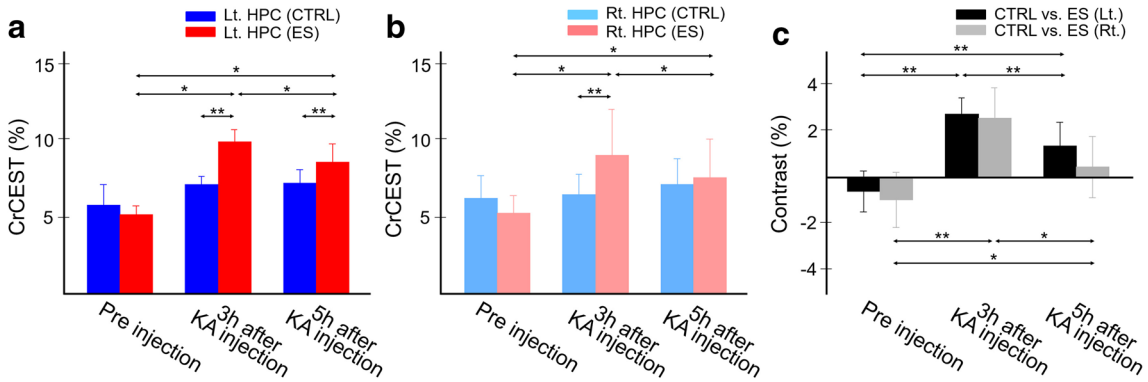

Fig. 2. Quantitative values of creatine CEST (CrCEST) between ES and CTRL groups at **a** left hippocampus, **b** right hippocampus, and **c** CrCEST signal contrasts between ES and CTRL groups at both hippocampus as a function of time after kainic acid (KA) injection. (Lt. HCP hippocampus at left hemisphere, Rt. HCP hippocampus at right hemisphere, ES epileptic seizure group by KA injection, and CTRL control group). $^{*}P < 0.05$, and $^{**}P < 0.005$.

creatine kinase, which serves to stabilize the effective reaction, leading to an increase in Cr. Because of these relationships, the epileptic mechanism can lead to a decrease in PCr and an increase in Cr. To demonstrate the metabolic change of Cr and PCr, ^{1}H MRS as used in this study and ^{31}P MRS would be the powerful and appropriate imaging.

However, the use of ^{31}P MRS in particular has some limitations, such as poor spatial resolution and sensitivity, and it is difficult to measure free Cr signal with sufficient accuracy [25, 26]. As an alternative to this issue, CEST has become widely used as a new MRI technique for indirect metabolite measurement using exchange-related properties; the signals of several metabolites, such as Cr, amide, amine, glucose, and glutamate, can be measured [29, 33–35].

By exploiting the features and merits of CrCEST technique, a hypothesis could be established. When the epilepsy occurs, change in the Cr signal in the hippocampus may also occur due to energy metabolism. As shown in results, it was available to detect signal changes using CrCEST imaging in KA-induced epilepsy model. Furthermore, by demonstrating the significant correlation between CrCEST and PCr and suggesting the reconstructed $CrCEST_{map}$, monitoring the signal changes of the Cr would be an important and useful factor to detect epileptic seizure in the rat model.

For the accuracy of ^{1}H MRS, we utilized a basis set, which can observe the concentration changes by LCModel, and performed a fully blind spectral analysis to minimize the bias. Based on our results, quantified CrCEST signals increased in the hippocampus after epilepsy onset, indicating an increase of Cr concentration. Furthermore, quantified PCr and tCR concentrations, using ^{1}H MRS analysis as a function of time, decreased and were not changed, respectively. As can be seen from the ATP synthesis relationship mentioned above, these phenomena can be explained by the complementary relationship between PCr and Cr, in which the concentration of Cr is increased to compensate for the decrease in the concentration of PCr in the energy metabolism relationship.

In addition, some previous literatures are concordant with our current results. DeFrance and McCandless produced a seizure state in rat and then measured key energy metabolites in hippocampal layers (stratum orierns, stratum pyramidale, and stratum radiatum) [36]. They showed that

Table 1. Summarized creatine signals (CrCEST) and contrast values between control (CTRL) and epileptic seizure (ES) groups at left and right hippocampus regions as a function of time, before and after kainic acid (KA) injection. All values are presented as means ± standard deviation. (Lt. HCP hippocampus at left hemisphere, and Rt. HCP hippocampus at right hemisphere)

		Pre KA injection		3 h after KA injection		5 h after KA injection	
		CTRL	ES	CTRL	ES	CTRL	ES
Lt. HPC	CrCEST (%)	5.8 ± 1.3	5.2 ± 0.6	7.1 ± 0.5	9.8 ± 0.8$^{(**)}$	7.2 ± 0.9	8.5 ± 1.2$^{(**)}$
		$\chi^2 = 10.000$; $P = 0.007$; *post-hoc*: all $P < 0.043^{(a)}$					
	Contrast (%)	−0.59 ± 0.88		2.73 ± 0.69		1.37 ± 1.01	
		$\chi^2 = 18.200$; $P = 0.000$; *post-hoc*: all $P < 0.007^{(a)}$					
Rt. HPC	CrCEST (%)	6.2 ± 1.4	5.3 ± 1.2	6.4 ± 1.3	8.9 ± 2.9$^{(**)}$	7.1 ± 1.7	7.5 ± 2.5
		$\chi^2 = 8.400$; $P = 0.015$; *post-hoc*: all $P < 0.043^{(a)}$					
	Contrast (%)	−0.96 ± 1.17		2.57 ± 1.30		0.44 ± 1.31	
		$\chi^2 = 13.400$; $P = 0.001$; *post-hoc*: all $P < 0.037^{(a)}$					

$^{**}P = 0.009$; Mann-Whitney *U* test between CTRL and ES groups, and [a]multiple comparisons using the non-parametric Friedman test between each time point at ES group

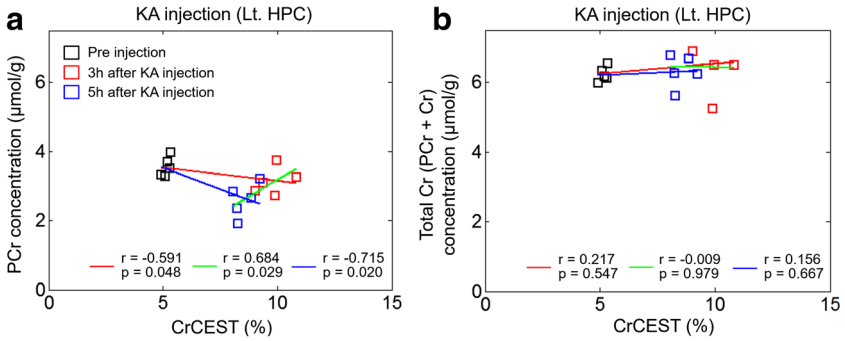

Fig. 3. Correlation analysis of creatine CEST (CrCEST) with **a** phosphocreatine (PCr) concentration and **b** total creatine (PCr + Cr) concentration at left hippocampus. Red line indicates the correlation between pre-KA injection and 3 h after kainic acid (KA) injection. Green line indicates the correlation between 3 and 5 h after KA injection. Blue line indicates the correlation between pre-KA injection and 5 h after KA injection. (r Spearman's rank correlation coefficient).

ATP and PCr were decreased significantly during the seizure state. In other words, producing overt seizures results in an increase in energy expenditure with resultant lowering of net level of key energy metabolites such as ATP and pCr. Other earlier *in vivo* NMR spectroscopy study found a significant decrease in PCr at hippocampus, followed by a plateau during the seizures in a rabbit [37]. In human clinical applications, two previous ^{1}H MRS studies have reported increase Cr level in the human temporal lobe epilepsy [38, 39].

This study was performed with a limited sample size, and utilized single-slice CrCEST imaging in the gross hippocampus region. However, it would be improved by increasing the number of samples with multiple cross-sectional CrCEST imaging analysis for measurements of the entire epilepsy network at the anatomical location of the hippocampus (dorsal, ventral, and cortical regions). Furthermore, in addition to the relationship of Cr/PCr, measuring the signal changes of α-, β-, and γ-ATP, which can be obtained using only ^{31}P MRS, will provide more meaningful information regarding ATP synthesis at the epileptic seizure stage in the future.

Conclusions

The CrCEST imaging showed significant image contrast at the stage of epileptic seizure, which was highly related with changes in creatine signals during energy consumption in the brain. The temporal evolution of the signal changes from CrCEST metric, and the evaluated correlations with PCr and total Cr results, clearly showed that CrCEST imaging can be a useful approach to estimate energy metabolism status in epilepsy.

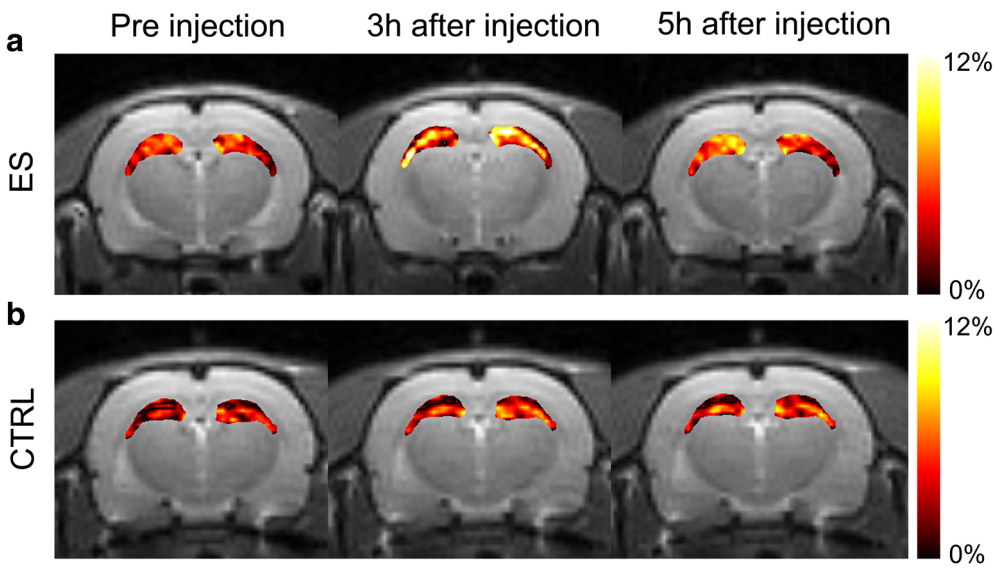

Fig. 4. Reconstructed creatine CEST (CrCEST) imaging of **a** epileptic seizure group and **b** control group for a typical rat, as a function of time after kainic acid injection.

Funding Information. This study was supported by grants of Basic Science Research Program through the National Research Foundation of Korea funded by the Ministry of Education [NRF (www.nrf.re.kr): NRF-2017R1A6A3A03012461 and NRF-2018R1A2B2007694] and the Korea Health Technology R&D Project through the Korea Health Industry Development Institute [KHIDI (www.khidi.or.kr): HI14C1090], funded by the Ministry of Health & Welfare, Republic of Korea.

Compliance with Ethical Standards

Conflict of Interest

The authors declare that they have no conflict of interest.

References

1. Holmes GL (2015) Cognitive impairment in epilepsy: the role of network abnormalities. Epileptic Disord 17:101–116
2. Mikati MA, Kurdit RM, Rahmeh AA et al (2004) Effects of creatine and cyclocreatine supplementation on kainate induced injury in pre-pubescent rats. Brain Inj 18:1229–1241
3. Tokumitsu T, Mancuso A, Weinstein PR, Weiner MW, Naruse S, Maudsley AA (1997) Metabolic and pathological effects of temporal lobe epilepsy in rat brain detected by proton spectroscopy and imaging. Brain Res 744:57–67
4. Tai XY, Bernhardt B, Thom M, Thompson P, Baxendale S, Koepp M, Bernasconi N (2018) Review: neurodegenerative processes in temporal lobe epilepsy with hippocampal sclerosis: clinical, pathological and neuroimaging evidence. Neuropathol Appl Neurobiol 44:70–90
5. Bernhardt BC, Fadaie F, Vos de Wael R, Hong SJ, Liu M, Guiot MC, Rudko DA, Bernasconi A, Bernasconi N (2017) Preferential susceptibility of limbic cortices to microstructural damage in temporal lobe epilepsy: a quantitative T1 mapping study. NeuroImage. https://doi.org/10.1016/j.neuroimage.2017.06.002
6. Deleo F, Thom M, Concha L et al (2017) Histological and MRI markers of white matter damage in focal epilepsy. Epilepsy Res 140:29–38
7. Ruber T, David B, Elger CE (2018) MRI in epilepsy: clinical standard and evolution. Curr Opin Neurol 31:223–231
8. Wong-Kisiel LC, Tovar Quiroga DF, Kenney-Jung DL, Witte RJ, Santana-Almansa A, Worrell GA, Britton J, Brinkmann BH (2018) Morphometric analysis on T1-weighted MRI complements visual MRI review in focal cortical dysplasia. Epilepsy Res 140:184–191
9. Fei P, Soucy JP, Obaid S et al (2018) The value of regional cerebral blood flow SPECT and FDG PET in Operculo-insular epilepsy. Clin Nucl Med 43:e67–e73
10. Jafari-Khouzani K, Elisevich K, Karvelis KC, Soltanian-Zadeh H (2011) Quantitative multi-compartmental SPECT image analysis for lateralization of temporal lobe epilepsy. Epilepsy Res 95:35–50
11. Long Z, Hanson DP, Mullan BP, Hunt CH, Holmes DR III, Brinkmann BH, O'Connor MK (2018) Analysis of brain SPECT images coregistered with MRI in patients with epilepsy: comparison of three methods. J Neuroimaging 28:307–312
12. Shiga T, Suzuki A, Sakurai K, Kurita T, Takeuchi W, Toyonaga T, Hirata K, Kobashi K, Katoh C, Kubo N, Tamaki N (2017) Dual isotope SPECT study with epilepsy patients using semiconductor SPECT system. Clin Nucl Med 42:663–668
13. Calabria FF, Cascini GL, Gambardella A et al (2017) Ictal ^{18}F-FDG PET/MRI in a patient with cortical heterotopia and focal epilepsy. Clin Nucl Med 42:768–769
14. Nardetto L, Zoccarato M, Santelli L, Tiberio I, Cecchin D, Giometto B (2017) ^{18}F-FDG PET/MRI in cryptogenic new-onset refractory status epilepticus: a potential marker of disease location, activity and prognosis? J Neurol Sci 381:100–102
15. House PM, Lanz M, Holst B, Martens T, Stodieck S, Huppertz HJ (2013) Comparison of morphometric analysis based on T1-and T2-weighted MRI data for visualization of focal cortical dysplasia. Epilepsy Res 106:403–409
16. Sone D, Sato N, Maikusa N, Ota M, Sumida K, Yokoyama K, Kimura Y, Imabayashi E, Watanabe Y, Watanabe M, Okazaki M, Onuma T, Matsuda H (2016) Automated subfield volumetric analysis of hippocampus in temporal lobe epilepsy using high-resolution T2-weighed MR imaging. Neuroimage Clin 12:57–64
17. Wolf OT, Dyakin V, Patel A, Vadasz C, de Leon MJ, McEwen BS, Bulloch K (2002) Volumetric structural magnetic resonance imaging (MRI) of the rat hippocampus following kainic acid (KA) treatment. Brain Res 934:87–96
18. Bartnik-Olson BL, Ding D, Howe J, Shah A, Losey T (2017) Glutamate metabolism in temporal lobe epilepsy as revealed by dynamic proton MRS following the infusion of [U-13-C] glucose. Epilepsy Res 136:46–53
19. Xu MY, Ergene E, Zagardo M, Tracy PT, Wang H, Liu WC, Machens NA (2015) Proton MR spectroscopy in patients with structural MRI-negative temporal lobe epilepsy. J Neuroimaging 25:1030–1037
20. Zahr NM, Crawford EL, Hsu O et al (2009) In vivo glutamate decline associated with kainic acid-induced status epilepticus. Brain Res 1300:65–78
21. Bessman SP, Carpenter CL (1985) The Creatine-Creatine phosphate energy shuttle. Annu Rev Biochem 54:831–862
22. Dulinska J, Setkowicz Z, Janeczko K, Sandt C, Dumas P, Uram L, Gzielo-Jurek K, Chwiej J (2012) Synchrotron radiation Fourier-transform infrared and Raman microspectroscopy study showing an increased frequency of creatine inclusions in the rat hippocampal formation following pilocarpine-induced seizures. Anal Bioanal Chem 402:2267–2274
23. Rambo LM, Ribeiro LR, Schramm VG, Berch AM, Stamm DN, Della-Pace ID, Silva LFA, Furian AF, Oliveira MS, Fighera MR, Royes LFF (2012) Creatine increases hippocampal Na(+), K(+)-ATPase activity via NMDA-calcineurin pathway. Brain Res Bull 88:553–559
24. Guivel-Scharen V, Sinnwell T, Wolff SD, Balaban RS (1998) Detection of proton chemical exchange between metabolites and water in biological tissues. J Magn Reson 133:36–45
25. Kogan F, Haris M, Debrosse C, Singh A, Nanga RP, Cai K, Hariharan H, Reddy R (2014) In vivo chemical exchange saturation transfer imaging of creatine (CrCEST) in skeletal muscle at 3T. J Magn Reson Imaging 40:596–602
26. Kogan F, Haris M, Singh A, Cai K, Debrosse C, Nanga RPR, Hariharan H, Reddy R (2014) Method for high-resolution imaging of creatine in vivo using chemical exchange saturation transfer. Magn Reson Med 71:164–172
27. Wolff SD, Balaban RS (1990) Nmr imaging of labile proton-exchange. J Magn Reson 86:164–169
28. Hellier JL, Patrylo PR, Buckmaster PS, Dudek FE (1998) Recurrent spontaneous motor seizures after repeated low-dose systemic treatment with kainate: assessment of a rat model of temporal lobe epilepsy. Epilepsy Res 31:73–84
29. Cai KJ, Haris M, Singh A, Kogan F, Greenberg JH, Hariharan H, Detre JA, Reddy R (2012) Magnetic resonance imaging of glutamate. Nat Med 18:302–306
30. Singh A, Cai KJ, Haris M, Hariharan H, Reddy R (2013) On B1 inhomogeneity correction of in vivo human brain glutamate chemical exchange saturation transfer contrast at 7T. Magn Reson Med 69:818–824
31. Tkac I, Starcuk Z, Choi IY, Gruetter R (1999) In vivo ^{1}H NMR spectroscopy of rat brain at 1 ms echo time. Magn Reson Med 41:649–656
32. Paxinos GWC (2007) The rat brain in stereotaxic coordinates, 6th edn. Elsevier Academic, London
33. Nasrallah FA, Pages G, Kuchel PW et al (2013) Imaging brain deoxyglucose uptake and metabolism by glucoCEST MRI. J Cereb Blood Flow Metabol 33:1270–1278
34. Zhang XY, Wang F, Li H, Xu J, Gochberg DF, Gore JC, Zu Z (2017) CEST imaging of fast exchanging amine pools with corrections for competing effects at 9.4 T. NMR Biomed 30:e3715. https://doi.org/10.1002/nbm.3715
35. Zhou J, Lal B, Wilson DA, Laterra J, van Zijl PCM (2003) Amide proton transfer (APT) contrast for imaging of brain tumors. Magn Reson Med 50:1120–1126

36. DeFrance JF, McCandless DW (1991) Energy metabolism in rat hippocampus during and following seizure activity. Metab Brain Dis 6:83–91
37. Petroff OA, Prichard JW, Behar KL et al (1984) In vivo phosphorus nuclear magnetic resonance spectroscopy in status epilepticus. Ann Neurol 16:169–177
38. Connelly A, Jackson GD, Duncan JS, King MD, Gadian DG (1994) Magnetic resonance spectroscopy in temporal lobe epilepsy. Neurology 44:1411–1417
39. Gadian DG, Connelly A, Duncan JS, Cross JH, Kirkham FJ, Johnson CL, Vargha-Khadem F, Nevile BG, Jackson GD (1994) ^{1}H magnetic resonance spectroscopy in the investigation of intractable epilepsy. Acta Neurol Scand Suppl 152:116–121